Dislocations Jam at Any Density

Georgios Tsekenis, Nigel Goldenfeld, and Karin A. Dahmen

Department of Physics, University of Illinois at Urbana-Champaign, Loomis Laboratory of Physics, 1110 West Green Street, Urbana, Illinois, 61801-3080, USA

(Received 20 November 2010; published 8 March 2011)

Crystalline materials deform in an intermittent way via dislocation-slip avalanches. Below a critical stress, the dislocations are jammed within their glide plane due to long-range elastic interactions and the material exhibits plastic response, while above this critical stress the dislocations are mobile (the unjammed phase) and the material flows. We use dislocation dynamics and scaling arguments in two dimensions to show that the critical stress grows with the square root of the dislocation density. Consequently, dislocations jam at any density, in contrast with granular materials, which only jam below a critical density.

DOI: 10.1103/PhysRevLett.106.105501 PACS numbers: 61.72.Hh, 61.72.Ff, 61.72.Lk, 62.20.fq

When a crystalline material is sufficiently deformed, it undergoes irreversible, or plastic deformation. Traditionally, plastic deformation of crystalline solids has been considered to be a smooth process in time, and homogeneous in space, since fluctuations are expected to average out at sufficiently large spatial scales. On small spatial scales, however, intermittent motion of dislocations is observed, resulting in a pattern of deformation that is spatially inhomogeneous and intermittent in time. This behavior is associated with a coherent motion of the dislocations that releases stress by slip avalanches: sequences of events with long-range correlations in space and in time. The slip avalanches span several orders of magnitude in size and the energy released is distributed according to a power law [1–6].

Theoretical models, including discrete dislocation dynamics models [1,7–11], continuum models [7,11–13], phase field models [11,14] and phase field crystal models [15] are able to reproduce many of the experimental findings and reveal scale invariant, power-law distributed phenomena that are indicative of a nonequilibrium critical point [16]. The dislocation system is jammed below a critical value of the external stress. Applying a constant external stress above the critical (yield) stress allows the system to flow, and the dislocations are unjammed. It is important to stress that in the glide plane of the dislocations, there is effectively no external potential, so that the jamming is an emergent phenomenon. However, recent work has shown that the behavior of the transition appears to be in the universality class of the interface pinning-depinning transition [11,15], as if there was an effective external potential induced by the collective interactions between the dislocations.

In this Letter we study connections between the plastic yield point of systems with long-range interactions, such as dislocation systems and the jamming transition of systems with short range interactions, such as sheared granular materials and molecular liquids [17–20]. When a system jams it undergoes a transition from a flowing state (analogous to a depinned phase) to a rigid state (analogous to a pinned phase). In contrast to the ordered solid phase obtainable via crystallization, the solid phase reached via jamming remains disordered. Liu and Nagel [17], O'Hern *et al.* [18,19], and others [20] studied jamming of granular materials with short range interactions in simulations and experiments. They found that below a critical density these materials do not jam at any stress. This critical density is called the jamming point J of granular materials. In contrast, we show here that dislocations jam at any nonzero density;, i.e., dislocations have no jamming point. The physical reason is that dislocations have long-range interactions that can lead to pinning for arbitrarily large distances between the dislocations. Figure 1 sketches the putative jamming phase diagram (in the absence of

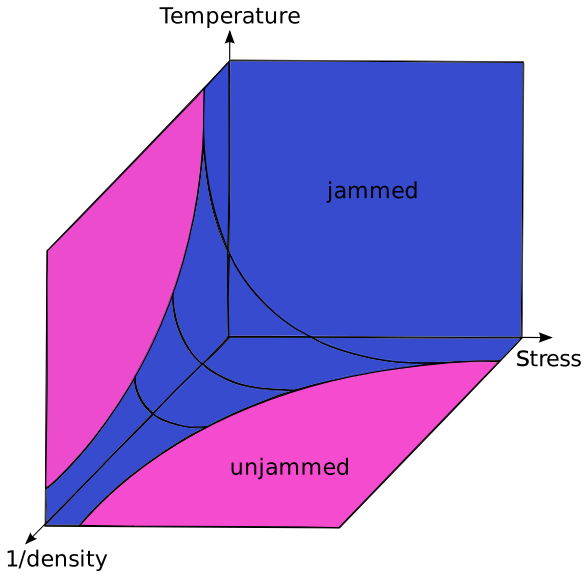

FIG. 1 (color online). Proposed phase diagram for dislocation systems. Notice the absence of a jamming point.

screening) for dislocation-mediated plasticity. It is closely related to the jamming phase diagram of [20] for granular materials, except for the absence of a jamming point J for dislocations.

In the following we employ analytical calculations and discrete dislocation dynamics simulations to study how the critical yield stress depends on the dislocation density ρ. Our analytical calculations verify and generalize the numerical findings.

The model.—We place N straight edge dislocations parallel to the z axis in a square box of side L. They are allowed to glide only along the shear direction (x axis), while they can interact in the x and y directions. This simulates a single-slip system. Materials, like ice, with strong plastic anisotropy, deform by glide on a single plane [1]. In these systems dislocation climb is negligible due to high plastic anisotropy. The z direction has been shown to be irrelevant to scaling [1,7–10] effectively rendering the problem two-dimensional. An edge dislocation with Burgers vector $\vec{b} = (b, 0)$ produces in the host medium an elastic shear stress at a distance $\vec{r} = (x, y)$,

$$\tau_{\rm int}(\vec{r}) = \frac{b\mu}{2\pi(1-\nu)} \frac{x(x^2-y^2)}{(x^2+y^2)^2}, \tag{1}$$

where μ is the shear modulus and ν is the Poisson ratio of the host medium [21]. This is anisotropic in the (x, y) plane and decays as $\tau_{\rm int} \sim 1/r$ at large $r = \sqrt{x^2+y^2}$. If an external shear stress $\tau_{\rm ext}$ is applied the overdamped equation of motion of a dislocation along the shear direction is described by,

$$\eta \frac{dx_i}{dt} = b_i \left(\sum_{j \neq i}^{N} \tau_{\rm int}(\vec{r}_j - \vec{r}_i) - \tau_{\rm ext} \right) \tag{2}$$

for $i, j = 1, \ldots, N$ where x_i is the x coordinate of the ith dislocation at point $\vec{r}_i$ with Burgers vector b_i, $\vec{r}_j$ with $j \neq i$ are the coordinates of the other $N-1$ dislocations, t is time and η is the effective viscosity in the host medium [1,7,8]. Here we have set the temperature to $T = 0$. For the computer simulations we have set the distance scale $b = 1$ and the time scale $t_0 = \eta/[\mu/(2\pi(1-\nu))] = 1$. To simulate bulk materials we employ periodic boundary conditions in both x and y directions.

To treat the long-range character of the dislocation interaction, we found the Lekner method [22] of image cells particularly straight forward. The equations of motion are solved by the adaptive-step fifth-order Runge-Kutta method [23]. The dislocation number is constant, since so far we considered neither dislocation creation nor annihilation. Equal numbers of dislocations with positive, $\vec{b} = +\hat{x}$, and negative, $\vec{b} = -\hat{x}$, Burgers vectors, render the system neutral. The dislocation collective speed (also called activity) $V(t)$, is defined as, $V(t) = \sum_{i=1}^{N} |v_i(t)|$ where $v_i = dx_i/dt$. The acoustic emission signal is proportional to the dislocation collective speed. Another popular choice is $V(t) = \sum_{i=1}^{N} b_i v_i(t)$, which is proportional to the strain rate [11].

Adiabatic increase of external stress.—First we consider the quasistatic or adiabatic case. After randomly placing the dislocations in the square cell, we let the system relax to the nearest (metastable) equilibrium state. During that procedure we apply zero external stress. As the system approaches the nearest energy minimum the dislocation motion slows down. A simple eigenmode analysis shows that the time needed for the system to reach zero activity diverges. We assume that the system is sufficiently close to the energy minimum when the dislocation activity has fallen below a threshold, $V_{\rm th} = 0.1$, which is roughly 100 times less than the initial activity of the $N = 64$ dislocation system. Once the system's activity has fallen below the specified threshold we start increasing the external stress adiabatically slowly. As soon as the adiabatically slowly increased stress pushes the system's activity above the threshold, $V(t) > V_{\rm th}$ and the system produces an avalanche, we keep the external stress constant until the avalanche stops (Fig. 2). The scaling behavior is insensitive

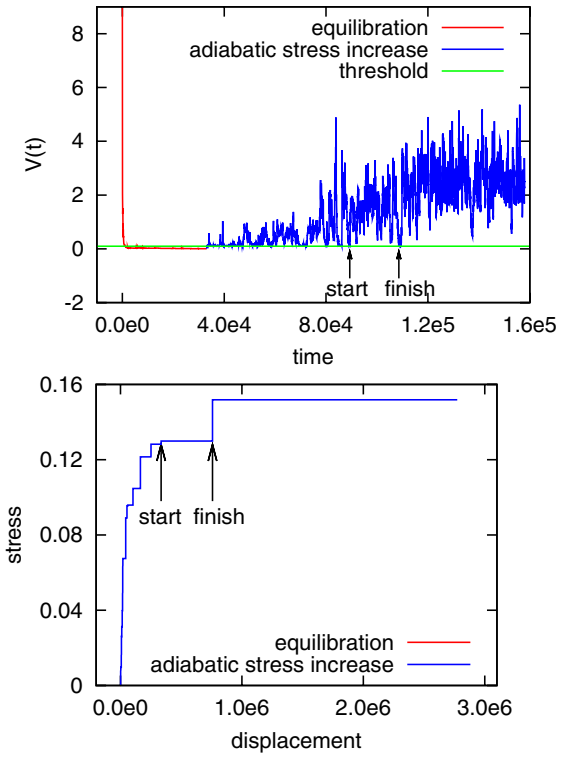

FIG. 2 (color online). (Top) Time dependence of the collective speed of all $N = 64$ dislocations in a square box of side $L = 100$. (Bottom) The stress plotted against the total dislocation displacement for the same run. Displacement at time t is the total distance all the dislocations traveled from the beginning of the simulation ($t = 0$) till time t: $\int_0^t dt' \sum_{i=1}^{N} b_i dx_i(t')$. The arrows indicate the start and finish of the last large avalanche. (Note that in the stress vs displacement bottom figure the equilibration occurs at zero external stress.)

to the threshold for a value up to 10 times larger and smaller.

The system starts with small avalanches and as the stress τ approaches the flow stress τ_c, it responds with larger and larger avalanches until at τ_c it finally flows steadily with an infinite avalanche. For $\tau > \tau_c$, the dislocations keep moving indefinitely, exiting from one side of the simulation cell and reemerging at the other due to the periodic boundary conditions, without ever getting jammed (pinned) again. In a deformation experiment, this is the point when the sample yields. In summary, for $\tau < \tau_c$ the system is jammed (pinned). For $\tau > \tau_c$ the system is constantly flowing (yielding) (Fig. 2).

Jamming.—The critical stress τ_c is not a universal quantity and every system with the same number of dislocations and box size has a different τ_c. We performed an adiabatically slow increase of the stress for different dislocation densities, $\rho = N/L^2$. The cumulative distributions of the critical stresses is shown in top Fig. 3. One can observe that the distributions become narrower for smaller densities, as does the mean critical stress of the ensemble. The scaling collapse shown in bottom Fig. 3 gives the relationship $\tau_c \sim \sqrt{\rho}$.

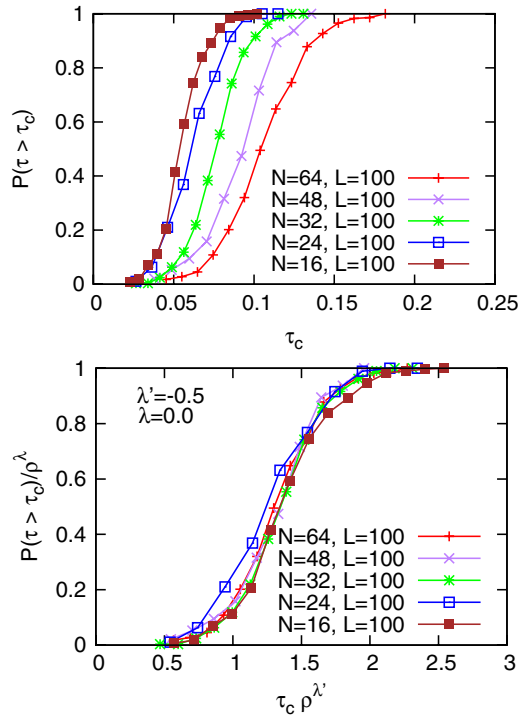

FIG. 3 (color online). (Top) The cumulative distribution of critical stresses τ_c for 5 different numerical densities. Each curve is extracted from 288 runs with $N = 64, 32, 16$ dislocations and 96 runs with $N = 48, 24$ dislocations in a square box of side $L = 100$. The smaller the density, the narrower the distribution and smaller the mean τ_c (see next Fig. 4). (Bottom) We obtain a good collapse using the curves with the three larger densities based on the expression $p(\tau_c, \rho) \sim \rho^{\lambda} f[\tau_c \rho^{\lambda'}]$. The collapse quantifies the fact that the distributions get steeper and have a smaller mean for lower density ρ. $\lambda = 0$ since the cumulative probability is restricted in $[0, 1]$. $\lambda' = -0.5 \pm 0.02$. The rescaling of the horizontal axis indicates that $\tau_c \sim \rho^{0.5}$.

The dislocation system exhibits jamming for $\tau < \tau_c$ analogous to the work of Liu and Nagel [17] and O'Hern *et al.* [18,19]. Their systems are different from ours in that they had exclusively short range interactions (contact interactions of soft spheres) and we have long-range (besides the core interactions that are enforcing the "no climb" constraint). They observed similar distributions of depinning stresses and a similar concave up dependence of the flow stress on the density (Fig. 4). However in contrast to their results, we neither expect nor find a jamming point equivalent to their jamming point J where $\tau_c = 0$. This means there can be no density, however small, that will unjam our system at zero applied external stress. The reason is that dislocations have long-range interactions [20]. No matter how far apart they are, they always feel each other.

Theoretical calculation of critical stress:—Consider $N^+_{R,\Delta R}$ positive and $N^-_{R,\Delta R}$ negative edge dislocations parallel to the z axis randomly distributed on a ring of radius R and thickness ΔR on the (x, y) plane. The stress exerted at the origin is given by

$$\tau_{R,\Delta R} = \int_R^{R+\Delta R} d^2 r \frac{\rho^+(r,\theta) - \rho^-(r,\theta)}{r} K(\theta), \quad (3)$$

adapted from [24], using Eq. (1) where $K(\theta) \sim \cos(\theta) \times \cos(2\theta)$ and $\rho^{\pm}(r,\theta) = \sum_{i=1}^{N^{\pm}_{R,\Delta R}} \frac{\delta(r-r_i)}{r^{d-1}} \delta(\theta - \theta_i)$. We express all distances in terms of l, the mean dislocation distance, i.e. $\rho = N/L^d = 1/l^d$ in d dimensions, i.e., $X = R/l$ and $x = r/l$. For any power-law $r^{-\alpha}$ interaction, we get $\tau_{X,\Delta X} = \frac{l^d}{l^\alpha} \int_X^{X+\Delta X} d^d x \frac{\rho^+(x,\theta) - \rho^-(x,\theta)}{x^\alpha} K(\theta)$ with $\rho^{\pm}(x,\theta) = \frac{1}{l^d} \sum_{i=1}^{N^{\pm}_{X,\Delta X}} \frac{\delta(x-x_i)}{x^{d-1}} \delta(\theta - \theta_i)$. For small ring

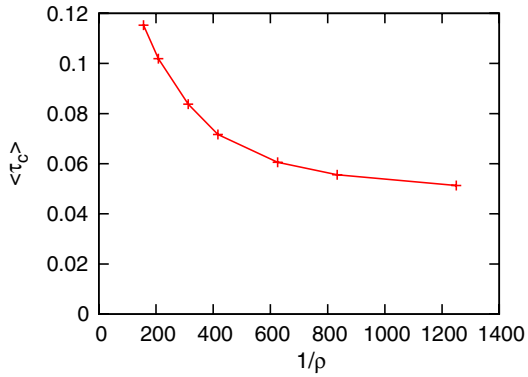

FIG. 4 (color online). The mean critical stress $\langle \tau_c \rangle$ plotted against the inverse numerical density ρ. The system is jammed for $\tau < \tau_c$ and unjammed above it. Each point is extracted from 288 runs with $N = 64, 32, 16, 8$ dislocations and 96 runs with $N = 48, 24, 12$ dislocations in a square box of side $L = 100$. The critical stress has a similar qualitative dependence on the density as in the proposed jamming phase diagram by Liu and Nagel [17]. However for dislocations $\tau_c(\rho) > 0$ for all nonzero densities ρ.

thickness we can approximate the integral with the value of the integrand at X times ΔX. The average over the number of the dislocations to first order gives

$$\langle \tau_{X,\Delta X} \rangle \sim \frac{1}{l^\alpha} \frac{\Delta X}{X^\alpha} (\langle N^+_{X,\Delta X} \rangle - \langle N^-_{X,\Delta X} \rangle) = 0 \qquad (4)$$

with $\langle N^+ \rangle = \langle N^- \rangle = \langle N \rangle$. The effect of the number fluctuations on the stress per ring thickness is

$$\left\langle \left(\frac{\tau_{X,\Delta X}}{\Delta X} \right)^2 \right\rangle \sim \frac{\langle (N^+_{X,\Delta X} - N^-_{X,\Delta X})^2 \rangle}{l^{2\alpha} X^{2\alpha}} \sim \frac{1}{l^{2\alpha}} \frac{\langle N_{X,\Delta X} \rangle}{X^{2\alpha}} \qquad (5)$$

since $N^\pm$ are independent random variables, Poisson distributed with the same mean and variance. Assuming that there are N dislocations of each kind in the entire area L^d where $X_L = L/l \gg 1$, their mean number in the ring can be expressed as $\langle N_{X,\Delta X} \rangle \sim N \frac{X^{d-1} \Delta X}{X_L^d}$. Substituting into Eq. (5) we find, $\langle (\frac{\tau_{X,\Delta X}}{\Delta X})^2 \rangle \sim \frac{1}{l^{2\alpha}} \frac{N}{X_L^d} \frac{\Delta X}{X^{2\alpha-d+1}}$ Integrating over the entire region,

$$\frac{\tau^2}{X_L^d} \equiv \int \left\langle \left(\frac{\tau_{X,\Delta X}}{\Delta X} \right)^2 \right\rangle \sim \frac{1}{l^{2\alpha}} \frac{N}{X_L^d} \int_{X_{\min}}^{X_L} \frac{dX}{X^{2\alpha-d+1}} \qquad (6)$$

with $X_{\min} \sim O(1)$ the closest possible distance between 2 dislocations gives $\frac{\tau}{\sqrt{N}} \sim \frac{1}{l^\alpha} \frac{1}{\sqrt{2\alpha-d}} \sqrt{\frac{1}{X_{\min}^{2\alpha-d}} - \frac{1}{X_L^{2\alpha-d}}}$ for $2\alpha > d$. In the thermodynamic limit, $X_L \to \infty$, this translates to the stress scaling as $\frac{\tau}{\sqrt{N}} \sim \frac{1}{l^\alpha} \sim \rho^{\alpha/d}$. For $2\alpha < d$, $\frac{\tau}{\sqrt{N}} \sim \frac{1}{l^\alpha} \times \frac{1}{\sqrt{d-2\alpha}} \sqrt{X_L^{d-2\alpha} - X_{\min}^{d-2\alpha}}$ and the thermodynamic limit does not exist. For parallel straight edge dislocations in 2 dimensions $2\alpha = d = 2$ and

$$\frac{\tau}{\sqrt{N}} \sim \frac{1}{l} \sqrt{\ln(L/l)} \sim \sqrt{\rho} \sqrt{\ln(L/l)}. \qquad (7)$$

This agrees with our numerical result in bottom Fig. 3. The extraction of logarithmic corrections requires much larger systems than the ones that can be simulated.

Discussion.—We were able to show, using a discrete dislocation dynamics model, that the mean critical stress of an ensemble of dislocation systems with long-range interactions, $\tau_{\text{int}} \sim 1/r$, scales with the square root of the dislocation density, $\langle \tau_c \rangle \sim \sqrt{\rho}$, for straight parallel edge dislocations. Equation (7) also agrees with the Taylor hardening relation [21] and is analogous to the effective velocity of a point vortex in 2 dimensional hydrodynamics [25]. We were able to perform the analytical calculation for any power-law interaction, $\tau_{\text{int}} \sim 1/r^\alpha$, and for arbitrary d dimensions. The theoretical result agrees with our simulation up to logarithmic corrections which are difficult to measure at system sizes amenable to simulation. Our results, both numerical and theoretical, show that for dislocations or particles with long-range interactions there can be no jamming point at a finite density (only at $\rho = 0$), provided there is no screening.

We thank M.-C. Miguel, M. Zaiser, J. Weiss, S. Zapperi, L. Laurson, M. Alava, D. Ceperley, V. Paschalidis, K. Schulten, R. Brunner, J. Estabrook, J. T. Uhl, Y. Ben-Zion, S. Papanikolaou, J. Sethna, B. Brinkman, L. Angheluta, H. Jaeger, A. Liu and S. Nagel for helpful conversations. We acknowledge NSF grant DMR 03-25939 ITR (MCC) and DMR 1005209, the University of Illinois Turing cluster, the KITP at UCSB (K. D.) and NSF grant TG-DMR090061 for TeraGrid TACC and NCSA resources.

[1] M.-C. Miguel, A. Vespignani, S. Zapperi, J. Weiss, and J. Grasso, Nature (London) **410**, 667 (2001).
[2] T. Richeton, P. Dobron, F. Chmelik, J. Weiss, and F. Louchet, Mater. Sci. Eng. A **424**, 190 (2006).
[3] T. Richeton, J. Weiss, and F. Louchet, Acta Mater. **53**, 4463 (2005).
[4] J. Weiss, F. Lahaie, and J. Grasso, J. Geophys. Res. **105**, 433 (2000).
[5] J. Weiss and J. Grasso, J. Phys. Chem. B **101**, 6113 (1997).
[6] D. Dimiduk, C. Woodward, R. LeSar, and M. Uchic, Science **312**, 1188 (2006).
[7] M. Zaiser, B. Marmo, and P. Moretti, Proc. Sci. SMPRI2005 (2005) 053.
[8] L. Laurson and M. J. Alava, Phys. Rev. E **74**, 066106 (2006).
[9] F. F. Csikor, C. Motz, D. Weygand, M. Zaiser, and S. Zapperi, Science **318**, 251 (2007).
[10] P. D. Ispanovity, I. Groma, G. Gyorgyi, F. F. Csikor, and D. Weygand, Phys. Rev. Lett. **105**, 085503 (2010).
[11] M. Zaiser, Adv. Phys. **55**, 185 (2006).
[12] M. Zaiser and P. Moretti, J. Stat. Mech. (2005) P08004.
[13] M. Zaiser and N. Nikitas, J. Stat. Mech. (2007) P04013.
[14] M. Koslowski, Philos. Mag. **87**, 1175 (2007).
[15] P. Y. Chan, G. Tsekenis, J. Dantzig, K. Dahmen, and N. Goldenfeld, Phys. Rev. Lett. **105**, 015502 (2010).
[16] J. Sethna, K. Dahmen, and C. Myers, Nature (London) **410**, 242 (2001).
[17] A. Liu and S. Nagel, Nature (London) **396**, 21 (1998).
[18] C. O'Hern, S. Langer, A. Liu, and S. Nagel, Phys. Rev. Lett. **88**, 7 (2002).
[19] C. O'Hern, L. Silbert, A. Liu, and S. Nagel, Phys. Rev. E **68**, 011306 (2003).
[20] A. Liu and S. Nagel, Annu. Rev. Condens. Matter Phys. **1**, 347 (2010).
[21] J. Hirth and J. Lothe, *Theory of Dislocations* (John Wiley and Sons, Inc., New York, 1982), 2nd ed.
[22] J. Lekner, Physica (Amsterdam) **176A**, 485 (1991).
[23] W. Press, S. Teukolsky, W. Vetterling, and B. Flannery, *Numerical Recipes in C: The Art of Scientific Computing* (Cambridge University Press, Cambridge, England, 1992), 2nd ed.
[24] I. Groma and B. Bako, Phys. Rev. B **58**, 2969 (1998).
[25] P. H. Chavanis, Phys. Rev. E **65**, 056302 (2002).